Oxygen plasma treatment of polystyrene and zeonor: substrates for adhesion of patterned cells

Beaulieu, Isabelle; Geissler, Matthias; Mauzeroll, Janine

Publisher's version / Version de l'éditeur:
https://doi.org/10.1021/la9001972
Langmuir, 25, 12, pp. 7169-7176, 2009-05-18

Langmuir
Article
pubs.acs.org/Langmuir

Oxygen Plasma Treatment of Polystyrene and Zeonor: Substrates for Adhesion of Patterned Cells

Isabelle Beaulieu,[†] Matthias Geissler,[‡] and Janine Mauzeroll*,[†]

[†]*Chemistry Department, Université du Québec à Montréal, 2101 Jeanne-Mance Street, Montreal, QC, H3C 3P8, Canada, and* [‡]*Industrial Materials Institute, National Research Council Canada, 75 de Mortagne Boulevard, Boucherville, QC, J4B 6Y4, Canada*

Received January 16, 2009. Revised Manuscript Received April 3, 2009

Plastic substrates made of polystyrene (PS) and Zeonor 1060R were treated with oxygen plasma to introduce polar groups (e.g., carbonyl and carboxylic acid) at the surface that render these materials hydrophilic and promote patterned adhesion of HeLa cells. Resultant surfaces were characterized using contact angle goniometry, atomic force microscopy (AFM), and X-ray photoelectron spectroscopy (XPS) to monitor changes in wettability, nanoscale topography, and chemical composition. Biocompatibility of the plastic surfaces was verified through fluorescence microscopy using three fluorophores, Alexa Fluor 488 conjugated to Annexin V, Hoechst 33258, and propidium iodide, indicating cells that undergo apoptosis and necrosis, respectively. The best cell growth was observed on PS treated at 5 W/sccm, for which the viability of adhering HeLa cells exceeded 90%. Patterning was accomplished using an elastomeric microcapillary system (μCS) made of poly(dimethylsiloxane) (PDMS) that consisted of a set of parallel channels to align cells in linear fashion. Densely populated bands were obtained on substrates of both plastic materials when the culture medium contained $> 2 \times 10^5$ cells/mL.

1. Introduction

Cells change their phenotype in response to their environment. Their metabolism, proliferation, and differentiation in adhering cultures are affected by several chemical cues that make it difficult to faithfully assign an in vitro gene expression and functional state with those that are present in vivo. Nevertheless, by learning to carefully control these cues, predictive cell-based assays could have a large impact on the early stages of drug discovery.[1] Adjustment of cell adhesion and proliferation conditions on solid supports is therefore important and has become central to a number of biotechnological areas, including single cell analysis, drug screening, and tissue engineering.[2,3] The work presented in this paper aims at exploring routine access to patterned cells on transparent, insulating substrates to be used in scanning electrochemical microscopy (SECM). SECM is an analytical technique that can be employed to assess cell viability,[4] monitor cell morphology,[5] and evaluate molecular transport through cell membranes with high sensitivity and resolution.[6,7] Continuing challenges in performing biological SECM studies include (i) limiting the use of serum-containing solutions during the SECM measurements to prevent tip fouling, (ii) restricting the experimental time to minimize exposure of cells to less than ideal growth conditions, and (iii) extending the scope of SECM measurements to cell communication studies.

In principle, cell growth can be achieved on a number of materials; yet, the preferred cell culture substrates are made from plastic polymers, such as polystyrene (PS), polycarbonate, and polyvinylchloride.[8,9] Pristine surfaces of most plastics are generally unsuitable for cell culture and therefore require modification. This can be achieved, for example, through exposure to gas plasma,[10] corona discharge,[11] or γ-irradiation,[8] followed by adsorption of molecules, which stimulate cell adhesion (also called attachment factors), such as fibronectin or collagen.[12] The adhesive molecule can be either physisorbed from the medium[13] or simply added to the surface[14] prior to adding the cell suspension. In the present study, we use physisorption from the serum, which is preferred over external deposition of attachment factors, as it reduces the number of manipulations required for cell patterning and allows for adhesion of cells within their preferred culture environment. Large deposits of single adhesion factors prior to incubation can also lead to reduced biological activity as a result of unfavorable conformational changes and restrict binding specificity to select cell-bound receptors.[15]

Most patterning schemes rely on microfabrication techniques in conjunction with surface modification to control adhesion, shape, and function of cells in a spatially defined manner.[3] For example, photolithography has been used to create structural

*To whom correspondence should be addressed. E-mail: mauzeroll.janine@uqam.ca.

(1) Bhadriraju, K.; Chen, C. S. *Drug Discovery Today* **2002**, *7*, 612–620.
(2) El-Ali, J.; Sorger, P. K.; Jensen, K. F. *Nature* **2006**, *442*, 403–411.
(3) Khademhosseini, A.; Langer, R.; Borenstein, J.; Vacanti, J. P. *Proc. Natl. Acad. Sci. U.S.A.* **2006**, *103*, 2480–2487.
(4) Kaya, T.; Torisawa, Y.-S.; Oyamatsu, D.; Nishizawa, M.; Matsue, T. *Biosens. Bioelectron.* **2003**, *18*, 1379–1383.
(5) Zhao, X.; Petersen, N. O.; Ding, Z. *Can. J. Chem.* **2007**, *85*, 1–183.
(6) Mauzeroll, J.; Bard, A. J.; Owhadian, O.; Monks, T. J. *Proc. Natl. Acad. Sci. U.S.A.* **2004**, *101*, 17582–17587.
(7) Sun, P.; Laforge, F. O.; Abeyweera, T. P.; Rotenberg, S. A.; Carpino, J.; Mirkin, M. V. *Proc. Natl. Acad. Sci. U.S.A.* **2008**, *105*, 443–448.
(8) Freshney, R. I. *Culture of Animal Cells. A Manual of Basic Technique*, 5th ed.; John Wiley & Sons: Hoboken, NJ, 2005; pp 105−113.
(9) Harrison, M. A.; Rae, I. F. *General Techniques of Cell Culture*; Cambridge University Press: New York, NY, 1997; pp 69−88.
(10) Strobel, M., Lyons, C. S., Mittal, K. L, Eds. *Plasma Surface Modification of Polymers: Relevance to Adhesion*; VSP: Utrecht, The Netherlands, 1994.
(11) Onyiriuka, E. C.; Hersch, L. S.; Hertl, W. *J. Colloid Interface Sci.* **1991**, *144*, 98–102.
(12) Folch, A.; Toner, M. *Annu. Rev. Biomed. Eng.* **2000**, *2*, 227–256.
(13) Kaji, H.; Tsukidate, K.; Hashimoto, M.; Matsue, T.; Nishizawa, M. *Langmuir* **2005**, *21*, 6966–6969.
(14) Folch, A.; Toner, M. *Biotechnol. Prog.* **1998**, *14*, 388–392.
(15) Benhabbour, S. R.; Sheardown, H.; Adronov, A. *Biomaterials* **2008**, *29*, 4177–4186.

information that can differentiate cell attachment.[16] Whitesides and co-workers have successfully confined cells on microcontact-printed self-assembled monolayers of alkanethiolates on gold.[17] It is also possible to deposit cells through a stencil that limits cell interactions to the exposed areas of the surface.[18] Finally, a number of approaches rely on laminar flow in microcapillary systems (μCSs), where adhesion-promoting ligands or cells can be confined at selected sites through hydrodynamic forces,[19] dielectrophoresis,[20] or the implementation of mechanical traps.[21] These systems are commonly (although not exclusively) fabricated from (PDMS) using rapid prototyping.[22] The use of this elastomer is favorable in part because of its ability to conform to other surfaces, resulting in a water-tight seal.[23] Fluidic cell patterning using PDMS-based devices has been applied to a wide range of cell types, including human umbilical vein[24] and bovine adrenal capillary[25] endothelial cells, human bladder cancer[25] cells, 3T3-J2 fibroblasts,[26] and Calu-3[27] and LLCPK1[24] epithelial cells.

The development of simple and efficient patterning schemes seems to be of vital importance for future SECM investigation, as it facilitates sample localization, reduces overall analysis time, and enables cell communication studies. For example, Matsue and co-workers showed that cell patterning helped evaluate cell respiration activity by SECM.[28] Herein, we investigate the conditions required for achieving patterned adhesion of living cells on two hard thermoplastic materials, Zeonor 1060R and PS from the serum and without additional attachment factors. Zeonor is an amorphous cyclo olefin copolymer that is produced using ring-opening metathesis of norbornene derivatives, followed by hydrogenation.[29] Unlike PS, this polymer is less frequently used as a cell culture substrate, even though it seems convenient to this end as it is inert, nontoxic, and has optical properties well-suited for transmission or fluorescence microscopy.[30,31] Moreover, Zeonor can be shaped using thermoforming processes (e.g., injection molding) or machined mechanically to custom-fabricate substrates of desired size and shape that can be adapted to biological SECM instrumentation. For the purpose of this study, we selected cancerous cervix epithelial (HeLa) cells, which are relatively robust and hence ideally suited for adhesion and patterning experiments.[32] We assessed the biocompatibility of the plastic surfaces using fluorescence microscopy in conjunction with fluorophores that stain cells undergoing apoptosis or necrosis. Fluorescence microscopy is preferable over viability tests based on flow cytometry[33,34] or laser scanning cytometry,[35] since it does not require detachment of the studied cells from the surface during electrochemical analysis.

2. Experimental Section

2.1. Preparation of Plastic Substrates. Zeonor and PS slides (25×75 mm^2 in area, 1 mm in thickness) were prepared by injection molding using a Boy 30A injection tool (Dr. Boy GmbH, Neustadt-Fernthal, Germany). Zeonor 1060R (Zeon Chemicals, Louisville, KY) was molded at a temperature of 250−260 °C, an injection speed of 40 mm/s, and a pressure of 132 bar. Molding of PS (MW = 100000, Alfa Aesar, Ward Hill, MA) was done at 195−205 °C, an injection speed of 30 mm/s, and a pressure of 132 bar. The mold (stainless steel, custom-fabricated) was cooled for 15 s before the slide was released. Slides were sonicated for three washing cycles of 10 min each, using methanol, ethanol, and deionized (DI) water (18.2 MΩ cm), respectively, to clean the surface of monomers or residual plasticizing agents. Slides were exposed to oxygen plasma (Plasmalab80Plus, Oxford Instruments, Bristol, United Kingdom) for 4 min at a pressure of 50 mTorr, and a power/gas flow ratio of between 0.5 and 100 W/sccm.

2.2. Surface Characterization. Contact angles were measured with a contact angle goniometer (model 200-F1) from Ramé-Hart Instrument Co. (Netcong, NJ) using DI water as the probe liquid. Images of advancing and receding drops were recorded with a CCD camera and analyzed using DROPimage Standard software. Roughness measurements on plastic surfaces were performed with a multimode Nanoscope IV atomic force microscope (Veeco Metrology Group, Santa Barbara, CA), operated at ambient conditions and in tapping mode using a silicon nitride cantilever (NCH Point Probe, Nanoworld, Neuchâtel, Switzerland) with a resonance frequency of 320 kHz and a spring constant of 42 N/m. For each sample, an area of 3×3 μm^2 was imaged at a rate of ~1.0 Hz, and a pixel resolution of 512×512. XPS spectra were recorded on a Kratos Analytical AXIS ULTRA spectrometer (Manchester, United Kingdom). The instrument was equipped with a hybrid lens and a monochromatic Al $K\alpha$ source (E = 1486.6 eV), providing a resolution of 0.4 eV. The analysis covered an area of 700×400 μm^2. Survey scans were collected between 1100 and 0 eV using an analyzer pass energy (PE) of 160 eV with 0.33 eV steps during 100 ms. High-resolution spectra were collected with a PE of 20 eV and steps of 0.1 eV during 200 ms for 8−40 scans. An electron flood gun was used to counterbalance charging of the insulating plastic surfaces during exposure. Elemental composition was calculated using Kratos instrument software Vision 2. Atomic concentrations were extracted from peak area calculations using a linear background with Scofield sensitivity factors and the instrument transmission functions.

2.3. Fabrication of μCSs. μCSs were prepared from PDMS (Sylgard 184, Dow Corning, Midland, MI) by curing a mixture (10:1 w/w) of elastomer base and cross-linker on a silicon/photoresist mold at 60 °C for at least 12 h. To fabricate the mold, a silicon wafer (Silicon Quest International, Inc., Santa Clara, CA) was first baked on a hot plate at 160 °C for 15 min before a layer of SU-8 (GM1040, Gersteltec, Pully, Switzerland) was applied through spin coating. This was followed by a prebake at 65 and 95 °C for 5 and 15 min, respectively, using a temperature ramp of 2 °C/min. The resist layer was exposed to UV light with a wavelength of 365 nm (Hg i-line) at 280 μJ/cm^2 through a quartz/Cr mask (HTA Photomask, San José, CA) using an

(16) Revzin, A.; Tompkins, R. G.; Toner, M. *Langmuir* **2003**, *19*, 9855–9862.
(17) Mrksich, M.; Dike, L. E.; Tien, J.; Ingber, D. E.; Whitesides, G. M. *Exp. Cell Res*. **1997**, *235*, 305–313.
(18) Park, T. H.; Shuler, M. L. *Biotechnol. Prog*. **2003**, *19*, 243–253.
(19) Takayama, S.; McDonald, J. C.; Ostuni, E.; Liang, M. N.; Kenis, P. J. A.; Ismagilov, R. F.; Whitesides, G. M. *Proc. Natl. Acad. Sci. U.S.A*. **1999**, *96*, 5545–5548.
(20) Voldman, J.; Gray, M. L.; Toner, M.; Schmidt, M. A. *Anal. Chem*. **2002**, *74*, 3984–3990.
(21) Wang, Z.; Kim, M.-C.; Marquez, M.; Thorsen, T. *Lab Chip* **2007**, *7*, 740–745.
(22) McDonald, J. C.; Whitesides, G. M. *Acc. Chem. Res*. **2002**, *35*, 491–499.
(23) Michel, B.; Bernard, A.; Bietsch, A.; Delamarche, E.; Geissler, M.; Juncker, D.; Kind, H.; Renault, J.-P.; Rothuizen, H.; Schmid, H.; Schmidt-Winkel, P.; Stutz, R.; Wolf, H. *IBM J. Res. Dev*. **2001**, *45*, 697–719.
(24) de Silva, M. N.; Desai, R.; Odde, D. J. *Biomed. Microdevices* **2004**, *6*, 219–222.
(25) Chiu, D. T.; Jeon, N. L.; Huang, S.; Kane, R. S.; Wargo, C. J.; Choi, I. S.; Ingber, D. E.; Whitesides, G. M. *Proc. Natl. Acad. Sci. U.S.A*. **2000**, *97*, 2408–2413.
(26) Folch, A.; Ayon, A.; Hurtado, O.; Schmidt, M. A.; Toner, M. *J. Biomech. Eng*. **1999**, *121*, 28–34.
(27) Mi, Y.; Chan, Y.; Trau, D.; Huang, P.; Chen, E. *Polymer* **2006**, *47* 5124–5130.
(28) Nishizawa, M.; Takoh, K.; Matsue, T. *Langmuir* **2002**, *18*, 3645–3649.
(29) Shin, J. Y.; Park, J. Y.; Liu, C.; He, J.; Kim, S. C. *Pure Appl. Chem*. **2005**, *77*, 801–814.
(30) Beattie, J. K. *Lab Chip* **2006**, *6*, 1409–1411.
(31) Mela, P.; van den Berg, A.; Fintschenko, Y.; Cummings, E. B.; Simmons, B. A.; Kirby, B. J. *Electrophoresis* **2005**, *26*, 1792–1799.
(32) Beaulieu, I.; Geissler, M.; Dansereau, D.; Mauzeroll, J. In *The Chemistry, Physics, and Engineering of Responsive Materials*; Bratcher, M. S., Gaddy, G. A., Kiserow, D., Maher, M. W., Eds.; John Wiley & Sons: Hoboken, NJ, in press.
(33) Cotter, T. G.; Al-Rubeai, M. *Trends Biotechnol*. **1995**, *13*, 150–155.
(34) Koopman, G.; Reutelingsperger, C. P.; Kuijten, G. A.; Keehnen, R. M.; Pals, S. T.; van Oers, M. H. *Blood* **1994**, *84*, 1415–1420.
(35) Taatjes, D.; Sobel, B.; Budd, R. *Histochem. Cell Biol*. **2008**, *129*, 33–43.

Table 1. Wetting Properties of PS Surfaces as a Function of Plasma Power

	< 1 h		24 h		9 days	
plasma power (W/sccm)	θ_{adv} (°)	θ_{rec} (°)	θ_{adv} (°)	θ_{rec} (°)	θ_{adv} (°)	θ_{rec} (°)
0	91 ± 2	71 ± 2	94 ± 2	75 ± 1	94 ± 1	77 ± 2
0.5	14 ± 2	< 10	28 ± 2	< 10	57 ± 2	18 ± 4
5	< 10	< 10	22 ± 4	< 10	41 ± 3	< 10
20	< 10	< 10	< 10	< 10	26 ± 8	< 10
40	< 10	< 10	< 10	< 10	15 ± 6	< 10
100	< 10	< 10	< 10	< 10	< 10	< 10

Table 2. Wetting Properties of Zeonor Surfaces as a Function of Plasma Power

	< 1 h		24 h		9 days	
plasma power (W/sccm)	θ_{adv} (°)	θ_{rec} (°)	θ_{adv} (°)	θ_{rec} (°)	θ_{adv} (°)	θ_{rec} (°)
0	97 ± 3	72 ± 6	94 ± 3	75 ± 3	100 ± 1	74 ± 1
0.5	26 ± 3	< 10	35 ± 2	12 ± 1	63 ± 2	23 ± 1
5	< 10	< 10	22 ± 7	< 10	50 ± 4	< 10
20	< 10	< 10	< 10	< 10	40 ± 4	< 10
40	< 10	< 10	< 10	< 10	36 ± 3	< 10
100	< 10	< 10	< 10	< 10	27 ± 3	< 10

EVG 6200 mask aligner (EV Group, Schärding, Austria). A postexposure bake was done using the same conditions as for the prebake. Resist features were developed in propylene glycol monomethyl ether acetate (Sigma-Aldrich Corp., St. Louis, MO) for 2 min. The wafer was then rinsed with isopropanol (Anachemia, Montreal, QC) and dried with a stream of nitrogen gas. The resultant resist pattern was hard-baked at 130 °C for 2 h. Finally, the master was coated with a thin, antiadhesive layer formed by exposure to 1*H*,1*H*,2*H*,2*H*-perfluorooctyl-trichlorosilane (Sigma-Aldrich) vaporized at reduced pressure. Inlets and outlets of channels were punched by hand upon release of the cured PDMS μCS from the mold.

2.4. Patterning of Cells. Mammalian cervix adenocarcinoma (HeLa) cells used for patterning were bought from ATCC (Manassas, VA). The cell culture medium, minimal essential medium containing L-glutamine (Invitrogen, Burlington, ON), was dissolved in nanopure water purified with a Millipore Milli-Q Biocel Ultrapure water system (Fisher, Ottawa, ON). The medium total volume contained 10% of fetal bovine serum (Invitrogen), 1% of a HYQ MEM nonessential amino acids solution 100× (HyClone, Logan, UT), and 1% of HYQ penicillin−streptomycin (10^4 units/mL, HyClone). The preparation was concluded by adding 1 mM sodium pyruvate and 2 mM sodium bicarbonate (biotechnology grade, BioShop Canada, Inc., Burlington, ON). The medium was vacuum filtered (Millipore 0.22 μm PES membrane filters, Fisher) before adding the amino acids and the serum that was already sterile. Cells were cultured in a 75 cm^2 growth area flask (Sarstedt, Inc., Saint-Leonard, QC) under a water-saturated atmosphere containing 5% CO_2. For patterning experiments, cells were detached from the culture flask with a solution of 0.25% w/v trypsin−0.26 mM EDTA−4Na (Sigma-Aldrich), suspended, and injected in the inlet of the PDMS μCS. Optimal cell adhesion required a 5 h resting period in the incubator prior to removal of the μCS.

2.5. Biocompatibility Tests. Alexa Fluor conjugated to Annexin-V (AV-Alexa Fluor 488) (λ_{ex} = 488 nm and λ_{em} = 520 nm) was purchased from Invitrogen, Bisbenzimide Hoechst 33258 (H33258) (λ_{ex} = 352 nm and λ_{em} = 461 nm) was obtained from Sigma-Aldrich, and propidium iodide (PI) (λ_{ex} = 535 nm and λ_{em} = 617 nm) was obtained from EMD Chemicals (Gibbstown, NJ). Each fluorescent probe tags cells during different stages of cell death. Selectivity to early apoptosis (AV-Alexa Fluor 488), late apoptosis (H33258), and necrosis (PI) was validated using tributyltin chloride (TBT, 96%, Sigma-Aldrich) and Triton X-100 surfactant (EMD Chemicals) serving as positive controls, respectively. First, cells were washed with phosphate-buffered saline (PBS, pH 7.4) prepared with PBS foil pouches (Sigma-Aldrich). Then, the first two fluorophores were added to the Petri dish containing the cells and binding buffer (HEPES, acid free, molecular biology grade, EMD Chemicals) and incubated for 15 min. After a second wash with PBS, PI was added prior to image acquisition.

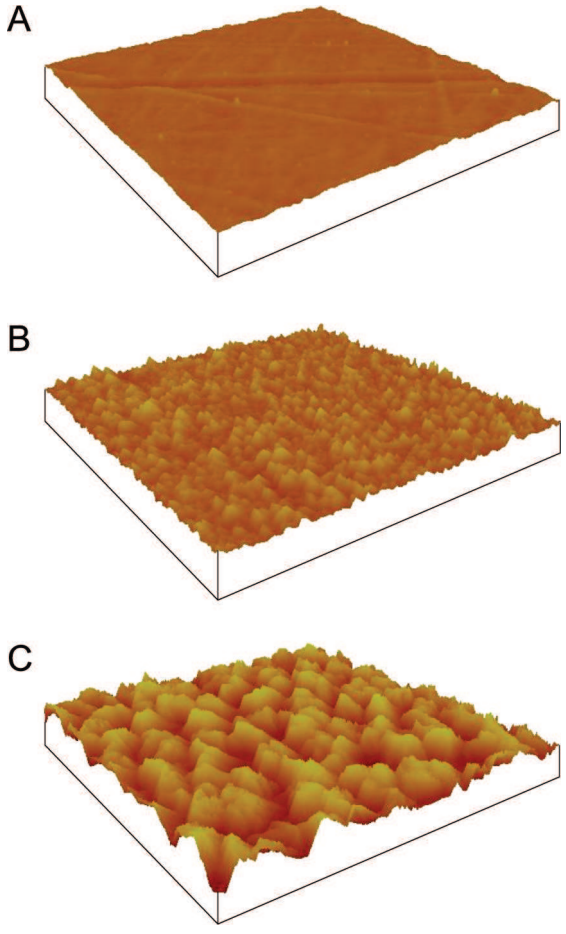

Figure 1. Surface topography of Zeonor 1060R substrates as revealed by AFM measurements. Images were taken from surfaces (A) in the pristine state and after exposure to oxygen plasma at (B) 5 and (C) 100 W/sccm. The scanned areas are 3 × 3 μm^2 for all examples; height scales are 50, 300, and 900 nm for images in A, B), and C, respectively.

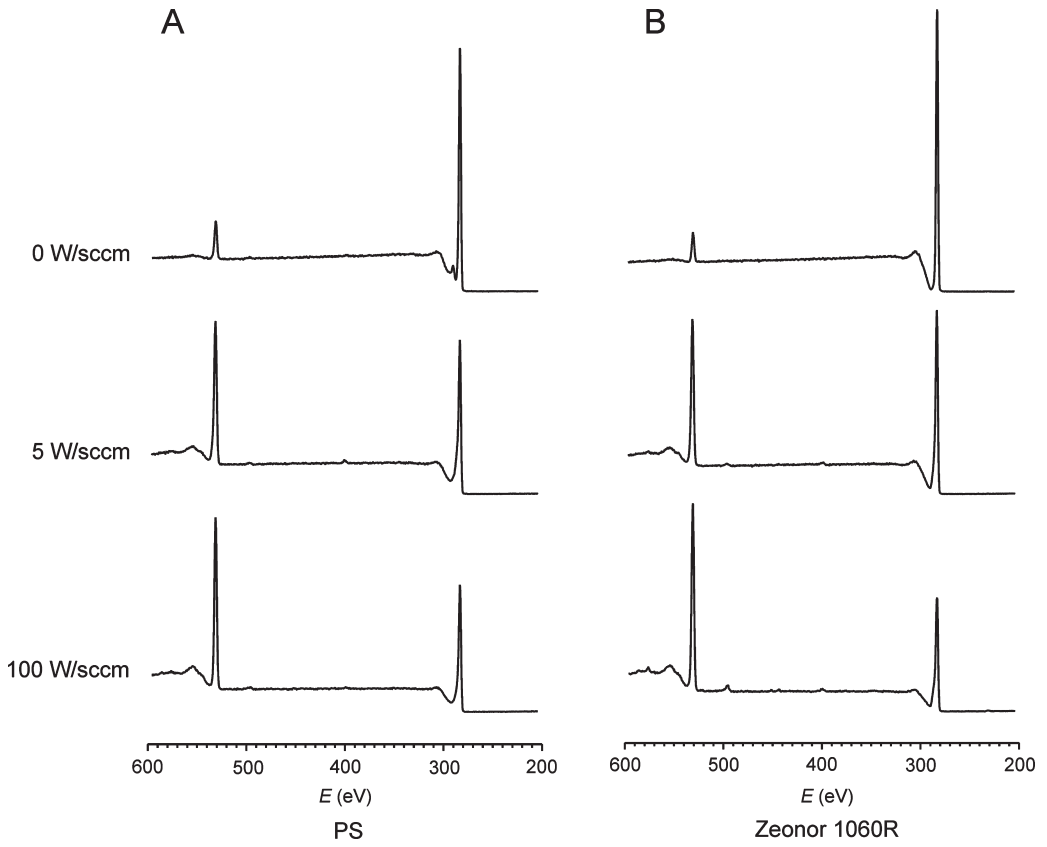

Figure 2. XPS survey spectra of (A) PS and (B) Zeonor 1060R substrates treated with O_2 plasma at 0, 5, and 100 W/sccm. Peak maxima for C 1s and O 1s are located at ~285 and 533.6 eV, respectively.

2.6. Optical and Fluorescence Imaging. Optical micrographs were obtained using a TS-100 microscope (Nikon, Montreal, QC) equipped with a Go-3 QImaging (Surrey, BC) camera using Q Capture Pro software (version 5.1). Fluorescence micrographs were acquired using a Nikon Eclipse TE2000-U inverted microscope equipped with an ultraviolet excitation filter block UV-2E/C, a green excitation filter block G-2A, and an endow GFP bandpass emission filter FGP(R)-BP (Nikon) using a Retiga 1300 CCD camera (QImaging) and Northern Eclipse software.

2.7. Flow Measurements. Two lines separated by a distance of ~1.0 mm were traced on the lower side of the plastic slides, serving as reference marks. The μCS contained three channels, each being 31 μm in height and 200 μm in width, which were aligned perpendicular to the underlying reference lines. Samples were placed on an Eclipse 50i microscope (Nikon) equipped with a CCD camera (Retiga 2000R Fast 1394 Mono Cooled, QImaging). Following injection of nanopure water into the inlet, the displacement of the fluid was captured on video using Nikon NIS-Element software (version 3.0). Liquid flow within capillaries was calculated from the velocity of the meniscus between the two reference lines.

3. Results and Discussion

3.1. Surface Analysis. Plasma exposure is an effective procedure to alter interfacial properties for a number of materials, most notably synthetic polymers. Depending on the composition of the ionizing gas, heteroatoms can be incorporated at the surface, thereby introducing functionality that affects wettability, surface charge, and adhesion. Treatment of plastic materials with oxygen plasma generally results in the formation of hydrophilic, oxygen-containing groups[36,37] (e.g., carbonyl, carboxyl, ester, etc.), which, in turn, increase the free energy[38] and promote wetting of the surface by polar solvents. As shown in Tables 1 and 2, pristine surfaces of both PS and Zeonor were hydrophobic with advancing contact angles (θ_{adv}) being $> 90°$.[39] As can be expected, surfaces of both materials became hydrophilic upon treatment with power/gas flow ratios larger than 0.5 W/sccm, resulting in advancing and receding (θ_{rec}) contact angles of $< 10°$. We noticed, however, that only exposure to plasma of high intensity (e.g., 100 W/sccm) yielded surfaces that were stable over longer periods of time (e.g., at least 9 days), while contact angles generally increased for all other conditions. Hydrophobic recovery of plasma-exposed polymers is a well-known phenomenon,[36] which is generally attributed to migration of low molecular weight residues along with rearrangement of polymer chains at the surface.

We inspected plastic surfaces using AFM to determine the impact of plasma intensity on micro- and nanoscale topography (Figure 1). Untreated samples displayed relatively smooth surfaces with a root-mean square (rms) roughness of ~0.5 nm. For both materials, rms roughness increased gradually with the power/gas flow ratio approaching values of ~25 nm upon exposure to 100 W/sccm. This finding is a result of decomposition and abrasive removal of material from the surface during treatment.[40] The increase in roughness, even though remaining restricted to the lower nanometer range, may contribute to the relatively large contact angle hysteresis[41]

(36) Morra, M.; Occhiello, E.; Garbassi, F. *Angew. Makromol. Chem.* **1991**, *189*, 125–136.
(37) Yasuda, H. *J. Macromol. Sci., Part A* **1976**, *10*, 383–420.
(38) Liston, E. M.; Martinu, L.; Wertheimer, M. R. In *Plasma Surface Modification of Polymers: Relevance to Adhesion*; Strobel, M., Lyons, C. S., Mittal, K. L., Eds.; VSP: Utrecht, The Netherlands, 1994; pp 3−39.
(39) Yasuda, T.; Okuno, T.; Yasuda, H. *Langmuir* **1994**, *10*, 2435–2439.
(40) Denes, F.; Young, R. A.; Sarmadi, M. *J. Photopolym. Sci. Technol.* **1997**, *10*, 91–112.
(41) Kwok, D. Y.; Neumann, A. W. *Adv. Colloid Interface Sci.* **1999**, *81*, 167–249.

Table 3. Atomic Concentration of Plasma-Treated Zeonor and PS Surfaces as Determined by XPS Measurements

	Zeonor 1060R				PS			
plasma power (W/sccm)	O (%)	N (%)	C (%)	others[a] (%)	O (%)	N (%)	C (%)	others[a] (%)
0	3.98	0.18	94.5	1.32	5.64	0.53	86.6	7.17
0.5	14.2	0.74	83.6	1.45	17.6	1.05	79.9	1.49
5	21.0	0.91	74.4	3.67	22.9	0.83	72.8	3.37
20	25.7	0.47	68.8	5.03	26.4	0.76	68.5	4.34
40	28.8	0.85	64.8	5.55	27.9	0.46	65.5	6.14
100	31.4	0.74	60.8	7.06	28.3	0.47	65.3	5.93

[a] Includes elements such as Na, Si, B, and Al at varying percentages.

that we observed when re-examining samples after a period of 9 days (see Tables 1 and 2).

The XPS spectra shown in Figure 2 reveal that exposure to O_2 plasma changes the relative peak intensities for C 1s and O 1s signals. Pristine surfaces of both PS and Zeonor are dominated by hydrocarbon (C−H) units that give rise to strong signal intensities at 285.0 eV. The appearance of a peak at 533.6 eV in these spectra accounts for ~4 and 5.6% of oxygen on Zeonor and PS surfaces, respectively (Table 3). Although it is possible that both polymer formulations include a certain degree of functionality within the network, it is likely that signals indicate the presence of oxygen-containing additives and/or molecules adsorbed at the surface while stored at ambient conditions. Upon treatment, the O 1s signal intensities increased progressively with the power/gas flow ratio, while C 1s signals decreased at the same time. The most drastic change was observed for Zeonor treated at 100 W/sccm, for which the atomic concentration of oxygen reached >31% (Table 3). As a consequence, the carbon content diminished from >94 to ~61%. The findings for PS, on the other hand, indicate saturation of the surface for plasma intensities >20 W/sccm, which is in good agreement with data reported in the literature.[42,43]

Deconvolution of high-resolution C 1s spectra (Figure 3) revealed a set of four distinct peaks (2−5) appearing as a result of the treatment process. The maximum of each peak was shifted toward higher energies with respect to the hydrocarbon signal at 285.0 eV (1), which is consistent with the formation of oxidized units in the polymer chains.[44,45] The example in Figure 3 illustrates the peak distribution for plasma-treated Zeonor using a standard fit algorithm. Peak (2) at 285.2 eV corresponds to carbon atoms next to an oxygen-containing group (e.g., C−CO_2), while peak (3) at 286.8 eV can be attributed to carbon atoms that are directly linked to one oxygen atom (C−O) as is the case for alcohols and ethers. Peak (4) at 288 eV reveals the presence of carbonyl groups (C═O) at the surface, yet may equally relate to carbon associated with two oxygen atoms (e.g., O−C−O). Peak (5) at 289.5 eV finally corresponds to carbon in acid and ester groups (O−C═O). The distribution of these peaks was prone to variation depending on the conditions of treatment; ratios on the other hand remained relatively stable over time. For example, after 20 days of storage, peak distribution for Zeonor treated at 100 W/sccm (Figure 3) was (1) 26.1%, (2) 49.1%, (3) 11.2%, (4) 8.1%, and (5) 5.5%. By comparison, the corresponding spectrum for PS revealed the following set of peaks: (1) at 285.0 eV, 37.6%; (2) 285.4 eV, 38.4%; (3) 287.4 eV, 12.2%; (4) 288.4 eV, 4.5%; and

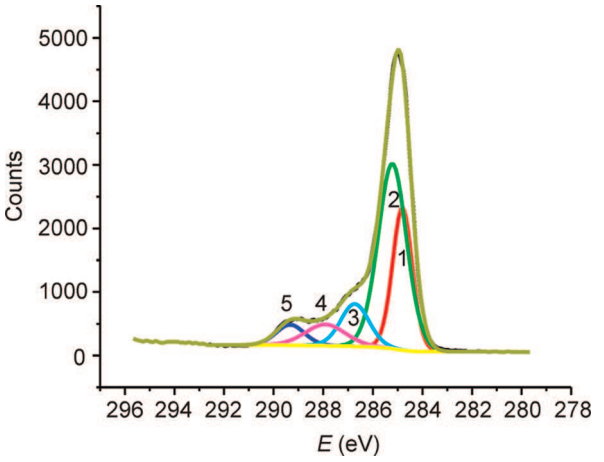

Figure 3. High-resolution spectrum of the C 1s signal of Zeonor 1060R treated with O_2 plasma at 100 W/sccm taken after 20 days upon exposure. Fit curves correspond to (1) C−H, (2) C−CO_2, (3) C−O, (4) O−C−O or C═O, and (5) O−C═O. See the text for details.

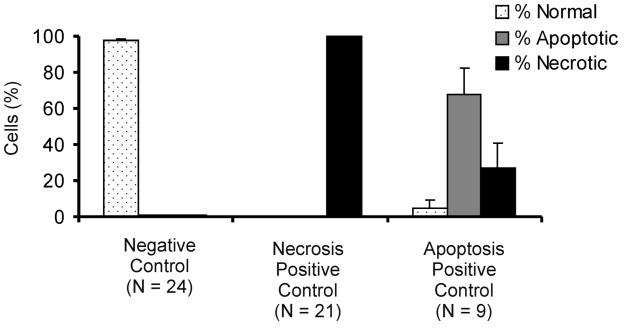

Figure 4. Necrotic and apoptotic cell death induced by Triton X-100 (0.075%) or tributyltin (2.0 μM), respectively, as revealed by fluorescence microscopy. HeLa cells were incubated with AV-Alexa Fluor 488 and H33258 in binding buffer for 15 min. Cells were washed with buffer, and PI was added prior to data acquisition.

(5) 289.7, 5.1%. In addition, the PS spectrum showed a shakeup energy peak at 291.8 eV,[36,46] accounting for 2.2% of the overall signal. These findings indicate that functional groups remain intact even over longer periods of time and hence should be suitable for cell patterning experiments.

3.2. Biocompatibility. Compatibility of the plastic substrates was probed using fluorescence microscopy in conjunction with dyes that tag cells in different stages of their dying process. We employed three commercially available fluorophores, AV-Alexa Fluor 488, H33258, and PI, whose selectivity toward apoptotic and necrotic cell death is presented in Figure 4. Analysis of variance statistical tests using $\alpha = 0.01$ from the Fisher−Snedecor distribution table[47]

(42) Johansson, B. L.; Larsson, A.; Ocklind, A.; Öhrlund, A. *J. Appl. Polym. Sci.* **2002**, *86*, 2618–2625.
(43) Larsson, A.; Ocklind, A. In *Polymer Surface Modification: Relevance to Adhesion*; Mittal, K. L., Ed.; VSP: Utrecht, The Netherlands, 2000; Vol. *2*, pp 121−135.
(44) Sakai, Y.; Norimatsu, H.; Saito, Y.; Inomata, H.; Mizuno, T. *Thin Solid Films* **2001**, *392*, 294–298.
(45) Diaz-Quijada, G. A.; Peytavi, R.; Nantel, A.; Roy, E.; Bergeron, M. G.; Dumoulin, M. M.; Veres, T. *Lab Chip* **2007**, *7*, 856–862.
(46) Shard, A. G.; Badyal, J. P. S. *J. Phys. Chem.* **1991**, *95*, 9436–9438.
(47) Scherrer, B. *Biostatistique*, 1st ed.; Gaëtan Morin Éditeur: Boucherville, QC, 1984.

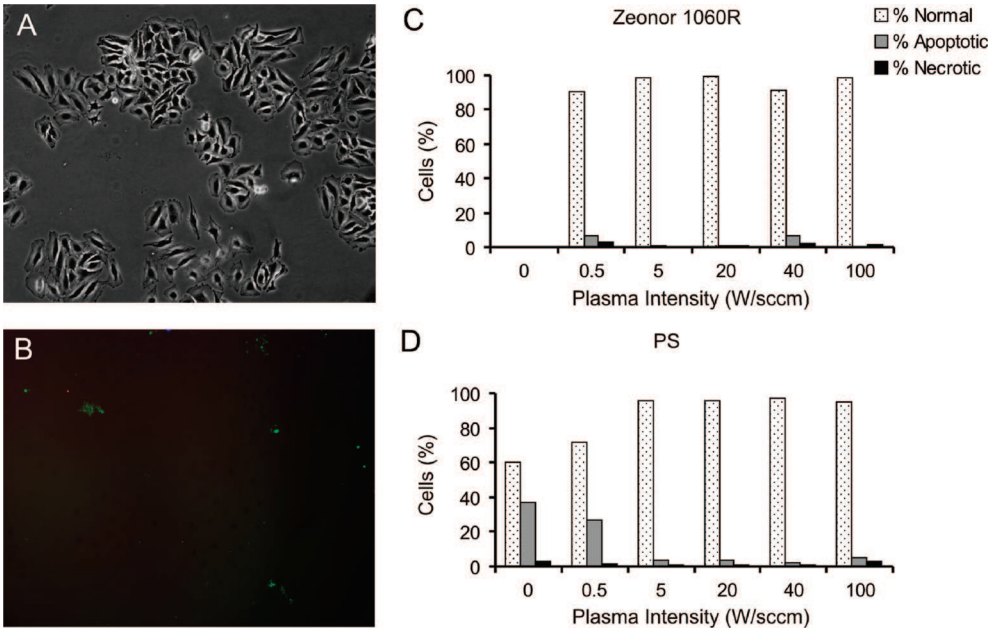

Figure 5. Biocompatibility of Zeonor and PS substrates as determined by fluorescence microscopy. (A) Optical micrograph of HeLa cells in binding buffer at pH 7.4 adhering to a Zeonor substrate treated with oxygen plasma at 5 W/sccm. Cells were incubated for 24 h. (B) Fluorescence micrograph of the same cells upon subsequent exposure to all three cell death indicators. AV-Alexa Fluor 488 and H33258 were incubated first; cells were washed with buffer after a period of 15 min, followed by addition of PI to the binding buffer. The absence of fluorescence signal indicates high viability of the population. (C and D) Quantification of cell viability on Zeonor and PS for different conditions of plasma treatment.

revealed that samples from all control experiments performed on different days could be considered as being part of the same statistical population. The negative control group represents cells untreated with a cell death inductor. Figure 4 shows that the majority of the cells remained untagged by the fluorophores, which corresponds to 98% of its population. Positive controls for necrosis consisted of cells exposed to 0.075% Triton X. This surfactant induces cell lysis and is often used to dissolve lipid membranes.[48] No variance was observed since 100% of the cells underwent necrosis, hence being tagged by PI. Upon incubation with TBT (here, 2 μM for 15 min), apoptosis[49,50] was observed for a large portion of cells in the corresponding control group. The data suggest some distribution in viability because the cell population is asynchronous and cells in the S phase (e.g., during DNA synthesis) are more vulnerable than others.[51] In the apoptosis positive control, AV-Alexa Fluor 488 and H33258 primarily tag apoptotic cells since the average numbers of apoptotic and necrotic cells are significantly different with $\alpha = 0.05$ from the Student distribution table.[47] AV-Alexa Fluor 488 and H33258 are therefore both adequate markers for cell apoptosis.

Figure 5 illustrates the biocompatibility of plastic substrates, which were incubated with HeLa cells over a period of four consecutive days. The images in Figure 5A,B reveal a typical cell population obtained on most plasma-treated surfaces. The absence of any notable fluorescence from cells is indicative of their proper metabolic functioning. As shown in Figure 5C, no cell growth was observed on pristine surfaces of Zeonor 1060R. Upon exposure to oxygen plasma, cells adhered on this plastic with normal cells exceeding 90% for any of the conditions used in this study. Figure 5D illustrates that it was possible to attach cells on pristine PS surfaces with ~60% viability of the population. In contrast to Zeonor, pristine PS is weakly charged, which likely favors cell adhesion.[52] Results for plasma-treated PS surfaces were largely comparable to those obtained for Zeonor. The relatively high percentage (e.g., 27%) of apoptotic cells in the case of samples treated at 0.5 W/sccm indicates that proper treatment of the surface is critical to the metabolic state of adhering cells.

3.3. Adhesion and Cell Growth on Plasma-Treated Surfaces. The serum used in this study contained fibronectin as a growth factor and adhesion promoter. Fibronectin is a protein that can associate with the collagen present in the extracellular matrix of a cell, which is considered to be a key event in the cell adhesion process.[43,52] We recorded the percentage of confluency in intervals of 24 h to verify progression of cell growth and proliferation on each substrate over a total period of 4 days (see Tables 4 and 5). Except for pristine Zeonor (Table 4), cells populated the surface of all samples, and confluency increased gradually over time. The highest confluency on Zeonor was 50%, corresponding to the substrate exposed at 0.5 W/sccm. For other conditions of treatment, confluencies varied between 23 and 37%. For PS (Table 5), few cells grew on the untreated surface, and little cell division (e.g., 7%) occurred during the period of observation. Substrates treated at 0.5 and 5 W/sccm showed the best rates of cell division (e.g., 80 and 60%, respectively), while confluency was on the order of 30% for all other samples. These trends are consistent with work performed by Larsson and co-workers on air plasma-treated substrates.[42] According to previous studies, good cell growth is obtained on less hydrophilic surfaces (e.g., $\theta_{adv} > 25°$). The relatively low contact angles that we obtained as a result of intense plasma treatment (see Tables 1 and 2) may partly explain the relatively poor confluency results for the

(48) Preté, P. S. C.; Malheiros, S. V. P.; Meirelles, N. C.; De Paula, E. *Biophys. Chem.* **2002**, *97*, 1–5.
(49) Zhu, X.; Xing, M.; Lou, J.; Wang, X.; Fu, W.; Xu, L. *Toxicology* **2007**, *230*, 45–52.
(50) Jurkiewicz, M.; Averill-Bates, D. A.; Marion, M.; Denizeau, F. *Biochim. Biophys. Acta, Mol. Cell Res.* **2004**, *1693*, 15–27.
(51) Kaufmann, W. K.; Paules, R. S. *FASEB J.* **1996**, *10*, 238–247.
(52) Saltzman, M. W. In *Principles of Tissue Engineering*; Lanza, R. P., Langer, R., Vacanti, J., Eds.; Academic Press: San Diego, CA, 2000; pp 221−235.

Table 4. Percentage of Cell Confluency on Zeonor Surfaces as a Function of Plasma Power

	confluency (%)			
plasma power (W/sccm)	24 h	48 h	72 h	96 h
0	0	0	0	0
0.5	8	25	37	50
5	8	17	22	23
20	8	12	23	29
40	6	12	25	35
100	6	15	30	37

Table 5. Percentage of Cell Confluency on PS Surfaces as a Function of Plasma Power

	confluency (%)			
plasma power (W/sccm)	24 h	48 h	72 h	96 h
0	5	8	9	7
0.5	5	37	63	80
5	<10	25	38	60
20	≥ 10	25	27	36
40	>10	18	22	25
100	20	20	25	30

corresponding samples. On the other hand, wettability does not seem to be the only criterion, since Zeonor samples often presented higher contact angles than PS with reduced cell confluency. Therefore, not only the surface itself but also the bulk properties of the polymer (e.g., its composition and morphology) may influence cell culture. The cell culturing capabilities of the treated plastics are, however, not a prerequisite for cell patterning. In the context of SECM analysis, pattern formation often implies the use of a larger concentration of cells, and confluency percentage is therefore not as important as if the plastics were modified solely for cell culture.

3.4. Cell Pattern Formation. The setup illustrated in Figure 6A accounts for an experimentally unsophisticated yet convenient fashion of confining cell assemblies to selected regions of a substrate. The μCS used for this study consisted of parallel channels, each connected to macroscopic access points (inlets and outlets, respectively) located at their extremities. The μCS is placed channel side down onto a plastic substrate; conformal contact seals the surface, and the embedded microcapillaries can be filled with liquid using capillary action, although the design is generally compatible with external pumping systems being connected to either inlets or outlets of the μCS. We validated the feasibility of this approach by estimating the velocity that can be reached by capillary force for water-based solutions on the plastic substrates without any treatment of the PDMS channels. Upon injection, displacement of water within the channels was observed in all cases except for plastics in their pristine forms, as can be expected from their respective advancing contact angles, which exceed 90° in both cases. For the samples exposed at 0.5 W/sccm, the probe liquid entered slowly, and the meniscus had an average velocity of <10 μm/s (see Experimental Section for details). For plastic substrates subjected to more intense plasma treatment, the velocity was substantially higher (e.g., >100 μm/s) because of their hydrophilic surfaces.

Capillary action was used to guide a suspension of cells in culture medium along the trajectories provided by the μCS, resulting in the formation of treads of immobilized cells on the plastic surface (Figure 6). We employed a culture medium that contained between 1 and 2.5×10^5 cells/mL in conjunction with an untreated μCS to ensure proper sealing of the surface and to limit cell attachment at the channel walls. Interestingly, for the concentrations $< 2 \times 10^5$ cells/ mL, almost no cells adhered on the plastic substrates. At high velocity, the cell suspension followed the fluid meniscus to the microchannel outlet, which provided limited interaction with the surface. For concentrations $> 2 \times 10^5$ cells/mL, we noticed that the reduced mobility of cells favored their interaction with the plastic slide once the flow was stopped, and the cells settled. It was therefore possible to attach cells on Zeonor (e.g., treated at 100 W/sccm) over the entire length of 400 μm wide microchannels (e.g., ~5 mm). We were able to obtain similar results for PS using comparable conditions of treatment (e.g., 40 and 100 W/sccm) and incubation (Figure 6B). We limited incubation time within the confined environment of microchannels to retain acceptable conditions for growth and proliferation, which primarily concerns the availability of oxygen and nutrition in the solution. Interestingly, the patterned assembly remained intact for extended periods of time (e.g., several days) once the μCS was removed from the substrate.

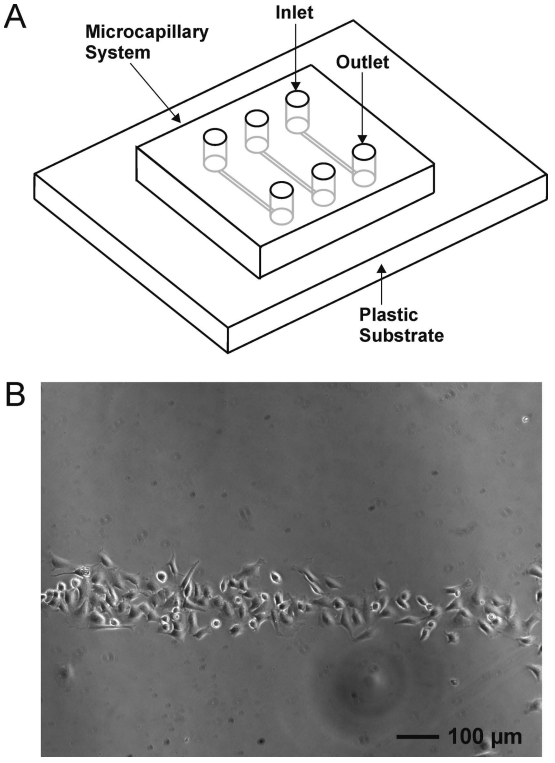

Figure 6. Patterning of cells within channels of a μCS. (A) Schematic of the PDMS device used for experiments. The height of channel was 27−31 μm, while their widths varied between 100 and 400 μm. (B) Optical micrograph of HeLa cells patterned on a PS surface treated with oxygen plasma at 40 W/sccm.

4. Conclusion

This study demonstrates that HeLa cells adhere on PS and Zeonor 1060R surfaces that have been hydrophilized using oxygen plasma at different power/gas flow ratios. Surface analysis proved useful to gain insight into chemical and morphological changes associated with this treatment process. Contrary to cell patterning strategies that rely on high concentrations of adhesion factors, cell attachment was promoted in part by the introduction of oxygen functionalities at the plastic surface. Patterning of cells on the functionalized substrates was achieved through the use of PDMS-based μCSs, although template-based patterning approaches may equally be useful to this end. While patterns generated on Zeonor surfaces showed well-separated cells along the trajectories that may be well-suited for single cell

measurements, assemblies on PS were more confluent and would be ideal to perform cell communication studies using SECM. The concentration of cells injected in the channels appeared to be an important parameter to the formation of cell patterns; here, optimized concentrations were on the order of 2×10^5 cells/mL. In producing cell patterns, care must be taken to limit PDMS debris and dust from entering the channel since they may cause adverse effects on the integrity of resultant patterns. Different cell delivery strategies along with variation in the design of the fluidic structures are presently being explored to further enhance reliability of the patterning process. We believe that the surface modification process presented in this study should also be compatible with a number of other cell lines, although experimental validation is yet to be achieved.

Acknowledgment. This work was supported by the National Science and Engineering Research Council of Canada and the Canadian Foundation for Innovation. We thank Dr. D. Karpuzov [Alberta Center for Surface Engineering and Science at the University of Alberta] for XPS analysis, and our colleagues D. Dansereau (UQÀM), T. Veres (IMI/NRC), H. Roberge (IMI/NRC), K.-M. Lau (IMI/NRC), and Prof. B. Annabi (UQÀM) for useful discussions and technical assistance.